

Resonance Raman and X-ray Crystallographic Studies of Intertriad Metal–Metal Bonds. 2. WRu and MoOs Porphyrin Dimers

James P. Collman,^{*,†} S. T. Harford,[†] Stefan Franzen,^{†,‡,§} Andrew P. Shreve,[‡] and William H. Woodruff[‡]

Department of Chemistry, Stanford University, Stanford, California 94305, and Los Alamos National Laboratory, Los Alamos, New Mexico 87545

Received August 25, 1998

Solution (¹H NMR, Evans method magnetic susceptibility, resonance Raman) and X-ray crystallographic spectroscopic studies of intertriad heterodimeric [(OEP)MoOs(OEP)] (**3**), [(OEP)WRu(OEP)] (**4**), [(OEP)MoOs-(TPP)]PF₆ (**5**⁺), and [(OEP)WRu(TPP)]PF₆ (**6**⁺) metalloporphyrins are reported (OEP = 2,3,7,8,12,13,17,18-octaethylporphyrinato; TPP = 5,10,15,20-tetraphenylporphyrinato). Evans method magnetic susceptibility data indicate that **3** and **4** contain two unpaired electrons in the ground electronic configuration. Resonance Raman spectra of **3**, **4**, **5**⁺, and **6**⁺ suggest that WRu bonds are 5–10% stronger than corresponding MoOs species. Structural characterization of **5**⁺ and **6**⁺ demonstrates metal–metal bond lengths of 2.30 (WRu) and 2.24 (MoOs) Å, respectively. The possibility of a special stability associated with polar heterometallic multiple bonds is discussed.

Introduction

Our recent successes in the preparation of intertriad heterometallic metal–metal-bonded complexes¹ have now been extended to the study of porphyrin dimers with W–Ru and Mo–Os multiple metal–metal bonds. An interesting component to the discussion of MoOs and WRu dimers is the effect of polarity on metal–metal bond length and strength. Until now such studies have only been possible between homodimers (Mo₂, W₂) and heterodimers (MoW) and have been complicated by the fact that the nonpolar species are axially symmetric (*D*_{4h}) while the polar species are not (*C*_{4v}), as well as the observation that the homodimers are composed of either two second-row metals or two third-row metals, while the heterodimer contains one of each.² For MoOs and WRu metal–metal-bonded dimers, both compounds are members of the same symmetry group, both contain one second-row metal and one third-row metal, and WRu is expected to be substantially more polar.³

The studies presented in this paper were conceived upon comparisons of X-ray diffraction and resonance Raman data for analogous homo- and heterodimers such as [Ru(TPP)]₂PF₆ (**1**⁺)⁴ and [(OEP)MoRu(TPP)]PF₆ (**2**⁺).^{1b} As discussed in the immediately preceding manuscript, **2**⁺ exhibits two structural isomers: one with porphyrin ligands eclipsed and an MO

diagram $\sigma^2\pi^4\delta^2\pi^{*1}$ (**2a**⁺) and one with staggered ligands and MO description $\sigma^2\pi^4\delta^{nb2}\pi^{*1}$ (**2b**⁺). Comparison of the MO diagram corresponding to **2b**⁺ with the MO diagram corresponding to [Ru(TPP)]₂PF₆ ($\sigma^2\pi^4\delta^2\delta^{*2}\pi^{*1}$) indicates that both **1**⁺ and **2b**⁺ exhibit metal–metal bonds of the same order and the same net composition (1 σ and 1.5 π bonds) with two 4d metals in the same oxidation states. Thus, one should expect comparable metal–metal bond lengths and metal–metal bond strengths. However, the X-ray structural data indicate a significantly shorter bond for the heterodimeric **2b**⁺ (2.18 vs 2.29 Å). Similarly, our immediately preceding discussion of [(OEP)WOs(OEP)] and [Os(OEP)]₂ reported a substantially higher force constant for the WOs⁴⁺ bond despite the fact that both are expected to exhibit homologous double bonds. Previously, researchers in this field have used these same criteria to propose a “special stability” inherent to heterometallic bonds upon comparison with analogous homodimers.⁵ To provide further insight into the effects of polarity on metal–metal bond length and strength, we have undertaken structural and vibrational studies of homologous MoOs and WRu porphyrin dimers and present our results herein.

Experimental Section

Materials. H₂OEP,⁶ H₂TPP,⁷ Mo(OEP)(PhC≡CPh),⁸ W(OEP)-(PEt₃)₂,⁹ Os(OEP or TPP)(pyridine)₂,¹⁰ and Ru(OEP or TPP)(pyridine)₂¹⁰ were synthesized according to published procedures. Diethylpyrrole was donated by Pharamcyclics and distilled immediately prior to use. Cobaltocene and ferrocenium hexafluorophosphate were purchased from

[†] Stanford University.

[‡] Los Alamos National Laboratory.

[§] Current address: North Carolina State University, Raleigh, NC 27695.

- (1) (a) Collman, J. P.; Arnold, H. J.; Weissman, K. J.; Burton, J. M. *J. Am. Chem. Soc.* **1994**, *116*, 9761–9762. (b) Collman, J. P.; Harford, S. T.; Marchon, J.-C.; Malidivi, P. *J. Am. Chem. Soc.* **1998**, *120*, 7999–8000.
- (2) (a) Luck, R. L.; Morris, R. H. *J. Am. Chem. Soc.* **1984**, *106*, 7978. (b) Collman, J. P.; Harford, S. T.; Franzen, S. F.; Eberspacher, T. A.; Shoemaker, R.; Woodruff, W. H. *J. Am. Chem. Soc.* **1998**, *120*, 1456–1465.
- (3) To a first approximation, Mo and Os are situated in the periodic table in a fashion analogous to O and Cl while the positions of W and Ru are analogous to those of S and F. Our initial approximation that WRu should therefore be more polar is supported by inspection of the Pauling electronegativities (see: Pauling, L. *The Nature of the Chemical Bond*; Cornell University Press: Ithaca, NY, 1960) as well as the ¹H NMR spectra of each complex. We have not been able to produce quantitative measurements of the dipole moments due to experimental difficulties in handling these compounds.

- (4) (a) Asahina, H.; Zisk, M. B.; Hedman, B.; McDevitt, J. T.; Collman, J. P.; Hodgson, K. O. *J. Chem. Soc., Chem. Commun.* **1989**, 1360–1362. (b) Tait, C. D.; Garner, J. M.; Collman, J. P.; Sattelberger, A. P.; Woodruff, W. H. *J. Am. Chem. Soc.* **1989**, *111*, 7806–7811. (c) Collman, J. P.; Prodollet, J. W.; Leidner, C. R. *J. Am. Chem. Soc.* **1986**, *108*, 2916–2921. (d) Collman, J. P.; Harford, S. T. *Inorg. Chem.* **1998**, *37*, 4152–4153.
- (5) Cotton, F. A.; Hanson, B. E. *Inorg. Chem.* **1978**, *17*, 3237.
- (6) Sessler, J. L.; Mozaffari, A.; Johnson, M. R. *Org. Synth.* **1992**, *70*, 68–77.
- (7) Adler, A. D.; Longo, F. R.; Finarelli, J. D.; Goldmacher, J.; Assour, J.; Korsakoff, L. *J. Org. Chem.* **1966**, *32*, 476.
- (8) De Cian, A.; Colin, J.; Schappacher, M.; Ricard, L.; Weiss, R. *J. Am. Chem. Soc.* **1981**, *103*, 1850–1851.

Strem and used as received. Benzene- d_6 and toluene- d_8 were purchased from Cambridge Isotope Laboratories and vacuum distilled from sodium benzophenone ketyl immediately prior to use. Solvents used for the metalation (decalin, chlorobenzene) and manipulation (benzene, toluene, hexanes, and dichloromethane) of the dimers were distilled from sodium benzophenone ketyl or P_2O_5 under argon before introduction into the glovebox.

Physical Measurements. A nitrogen-filled Vacuum Atmospheres drybox equipped with a Dri-Train inert-gas purifier was employed for manipulations carried out under anaerobic conditions. 1H NMR spectra were recorded on a Varian XL-400 or Varian-Oxford 500 MHz FT-NMR spectrometer using benzene- d_6 or toluene- d_8 as a solvent. Resonances in the 1H NMR were referenced versus the residual proton signal of the solvent.

Resonance Raman samples were prepared in the glovebox and flame sealed under vacuum. Excitation for the RR experiments was provided by an Ar^+ ion laser (Spectra Physics). Typical laser powers were 20–30 mW on resonance. Scattered light was collected by an $f/1$ 5 cm focal length lens and focused onto the slit of a SPEX 0.6 operating as a spectrograph to disperse the light onto a Photometrics CCD camera. Typical data acquisition times were 20 min. Because the precision of the depolarization ratios (ρ) was ± 0.1 , only general information such as whether bands were polarized (a_{1g} modes), depolarized (b_{1g} and b_{2g}), or anomalously polarized (a_{2g}) could be determined. Sample integrity following irradiation was confirmed by 1H NMR and electronic absorption spectroscopy.

Crystals of the [(OEP)WRu(TPP)]PF₆ dimer suitable for X-ray diffraction were obtained by vapor diffusion of benzene into a saturated dichloromethane solution. A lustrous blue crystal with dimensions $0.20 \times 0.20 \times 0.01$ mm was chosen and mounted on a glass fiber in paratone N oil at -80 °C using an improvised cold stage. The same method was also used to mount a $0.30 \times 0.30 \times 0.007$ mm crystal of [(OEP)MoOs(TPP)]PF₆ grown by layering of a dichloromethane solution with pentane. All measurements were made on a Siemens SMART diffractometer with graphite-monochromated Mo K α radiation.

Both structures were solved by direct methods (SHELXS-86) and expanded using Fourier techniques (DIRDIF92). All Mo, Ru, Os, W, P, F, and Cl atoms were refined anisotropically. Carbon and nitrogen atoms were refined isotropically. With hydrogen atoms included at idealized positions, the final cycle of full-matrix least-squares refinements converged to $R = \sum |F_o| - |F_c| / \sum |F_o| = 0.109$ (MoOs) and 0.072 (WRu) and $R_w = [(\sum w(|F_o| - |F_c|)^2) / \sum w F_o^2]^{1/2} = 0.134$ (MoOs) and 0.088 (WRu).

Preparation of [(OEP)MoOs(OEP)] (3). Vacuum pyrolysis of a mixture of Mo(OEP)(PhC \equiv CPh) (23.8 mg) and Os(OEP)(py)₂ (23.2 mg) at 6×10^{-6} Torr and 210 °C (4 h) yields 33.1 mg of a mixture of 18% [Mo(OEP)]₂, 73% [(OEP)MoOs(OEP)], and 8% [Os(OEP)]₂. Isolation of the mixed species is effected by redox titration exactly as prescribed below in the preparation of **4**. The yield of [(OEP)MoOs(OEP)] is 15.2 mg, 42.0%.

UV-vis [nm (log ϵ): Soret Os(OEP) 358 (4.46), Soret Mo(OEP) 396 (4.72). 1H NMR (ppm, C₆D₆): δ -67.92 (s, 4H, Mo H_{meso}); -50.93 (s, 4H, Os H_{meso}); 20.36 (m, 8H, Mo-CH₂CH₃), 16.72 (m, 8H, Mo-CH₂CH₃); 10.31 (m, 8H, Os-CH₂CH₃), 9.20 (m, 8H, Os-CH₂CH₃); 0.20 (t, 24H, Mo-CH₂CH₃); 0.87 (t, 24H, Os-CH₂CH₃). μ_{eff} (toluene- d_8): 2.72 μ_B . Mass spectrum, LSIMS (CsI calibration): simulated (relative intensity), 1342.4 (1.00), 1343.4 (0.99), 1344.4 (0.99), 1341.4 (0.93), 1340.4 (0.78), 1345.4 (0.71), 1339.4 (0.59); found (relative intensity), 1342.1 (1.00), 1343.1 (0.99), 1344.1 (0.98), 1341.1 (0.92), 1340.1 (0.79), 1345.1 (0.76), 1339.1 (0.59).

Preparation of [(OEP)WRu(OEP)] (4). Vacuum pyrolysis of a mixture of W(OEP)(PEt₃)₂ (29.1 mg) and Ru(OEP)(py)₂ (21.2 mg) at 6×10^{-6} Torr and 210 °C (4 h) yields 35.1 mg of a mixture of 16% [W(OEP)]₂, 32% [(OEP)WRu(OEP)], 48% Ru(OEP)(PEt₃)₂, and 4% [Ru(OEP)]₂.

Oxidation. In a nitrogen-atmosphere glovebox, the reaction mixture is dissolved in benzene (7 mL); to this is added Cp₂FePF₆ (4.4 mg, 13.3 μ mol, 0.75 equiv relative to [(OEP)WRu(OEP)]). The mixture is stirred overnight and then filtered through Celite. The precipitate is rinsed with benzene and then eluted with dichloromethane. The solution is concentrated under vacuum to yield [(OEP)WRu(OEP)]PF₆.

Reduction. To this solid is added an excess of Cp₂Co^{II} in benzene (5 mL) and stirred for 4 h. The solution is concentrated while heating under vacuum to remove unreacted Cp₂Co and side product Cp₂CoPF₆. The residual solid is analytically pure [(OEP)WRu(OEP)]; neither of the homodimers is observed in either the 1H NMR or mass spectrum. The yield of [(OEP)WRu(OEP)] is 7.6 mg, 59.6%.

UV-vis [nm (log ϵ): Soret Ru(OEP) 360 (4.66), Soret W(OEP) 396 (4.86), 520 (4.16), 568 (4.20). 1H NMR (ppm, C₆D₆): δ -90.0 (s, 4H, W H_{meso}); -16.10 (s, 4H, Ru H_{meso}); 23.90 (m, 8H, W-CH₂CH₃), 20.45 (m, 8H, W-CH₂CH₃); 7.08 (m, 8H, Ru-CH₂CH₃), 6.40 (m, 8H, Ru-CH₂CH₃); -0.80 (t, 24H, W-CH₂CH₃); 1.95 (t, 24H, Ru-CH₂CH₃). μ_{eff} (toluene- d_8): 2.80 μ_B . Mass spectrum, LSIMS (CsI calibration): simulated (relative intensity), 1350.6 (1.00), 1349.6 (0.85), 1351.6 (0.81), 1352.6 (0.80), 1348.6 (0.75), 1347.6 (0.51); found (relative intensity), 1350.9 (1.00), 1351.9 (0.82), 1349.9 (0.80), 1348.8 (0.77), 1352.9 (0.75), 1347.8 (0.55).

Preparation of [(OEP)WRu(TPP)] (5). Vacuum pyrolysis of a mixture of W(OEP)(PhC \equiv CPh) (35 mg) and Ru(TPP)(py)₂ (25 mg) at 6×10^{-6} Torr and 210 °C (4 h) yields 32 mg of a mixture of 14% [W(OEP)]₂, 78% [(OEP)WRu(TPP)], and 8% [Ru(TPP)]₂. Isolation of the mixed species is effected by redox titration exactly as described above in the preparation of **4**. The yield of [(OEP)WRu(TPP)] is 11.0 mg, 46.5%.

UV-vis [nm (C₆H₆, log ϵ): Soret Ru(TPP) 371 (4.63), Soret W(OEP) 391 (4.89). 1H NMR (ppm, C₆D₆): δ -74.2 (s, 4H, W H_{meso}); -5.8 (s, 8H, Ru H_B); 20.10 (m, 8H, W-CH₂CH₃), 23.31 (m, 8H, W-CH₂CH₃); 7.19 (d, 4H, Ru endo *o*-phenyl), 8.65 (t, 4H, Ru endo *m*-phenyl); 5.75 (d, 4H, Ru exo *o*-phenyl), 6.25 (t, 4H, Ru exo *m*-phenyl); 7.35 (t, 4H, Ru *p*-phenyl); -0.20 (t, 24H, W-CH₂CH₃). Mass spectrum, LSIMS (CsI calibration): simulated (relative intensity), 1430.5 (1.00), 1429.5 (0.85), 1431.5 (0.84), 1432.5 (0.82), 1428.5 (0.74), 1433.5 (0.50), 1427.5 (0.49); found (relative intensity), 1429.6 (1.00), 1428.6 (0.88), 1430.6 (0.84), 1431.6 (0.81), 1427.6 (0.77), 1426.7 (0.54), 1432.7 (0.51).

Preparation of [(OEP)MoOs(TPP)] (6). Vacuum pyrolysis of a mixture of Mo(OEP)(PhC \equiv CPh) (20 mg) and Os(TPP)(py)₂ (21 mg) at 6×10^{-6} Torr and 210 °C (4 h) yields 23 mg of a mixture of 23% [Mo(OEP)]₂, 65% [(OEP)MoOs(TPP)], and 11% [Os(TPP)]₂. Isolation of the mixed species is effected by redox titration exactly as described above in the preparation of **4**. The yield of [(OEP)MoOs(TPP)] is 10.4 mg, 39.6%.

UV-vis [nm (C₆H₆, log ϵ): Soret Os(TPP) 359 (4.65), Soret Mo(OEP) 399 (4.93). 1H NMR (ppm, C₆D₆): δ -32.5 (s, 4H, Mo H_{meso}); 1.21 (s, 8H, Os H_B); 14.15 (m, 8H, Mo-CH₂CH₃), 17.82 (m, 8H, Mo-CH₂CH₃); 9.80 (d, 4H, Os endo *o*-phenyl), 8.10 (t, 4H, Os endo *m*-phenyl); 6.95 (d, 4H, Ru exo *o*-phenyl), 7.51 (t, 4H, Os exo *m*-phenyl); 7.95 (t, 4H, Ru *p*-phenyl); 1.01 (t, 24H, Mo-CH₂CH₃). Mass spectrum, LSIMS (CsI calibration): simulated (relative intensity), 1432.5 (1.00), 1431.5 (0.91), 1430.5 (0.82), 1433.5 (0.79), 1434.5 (0.78), 1429.5 (0.70), 1428.5 (0.61); found (relative intensity), 1431.5 (1.00), 1432.5 (0.98), 1433.5 (0.93), 1430.5 (0.92), 1429.5 (0.86), 1434.5 (0.70), 1428.5 (0.68).

Results and Discussion

1H NMR. Chemical shift and Evans method¹¹ magnetic susceptibility data for [(OEP)MoOs(OEP)] (**3**), [(OEP)WRu(OEP)] (**4**), and [Re(OEP)]₂ are presented in Table 1. In fashion similar to the NMR results presented for MoRu and WO os dimers, the data in Table 1 suggested a paramagnetic ground electronic configuration, $\sigma^2\pi^4\delta^2\pi^*2$, to be in effect for the heterodimers **3** and **4**.

(9) Collman, J. P.; Garner, J. M.; Woo, L. K. *J. Am. Chem. Soc.* **1989**, *111*, 8141–8148.

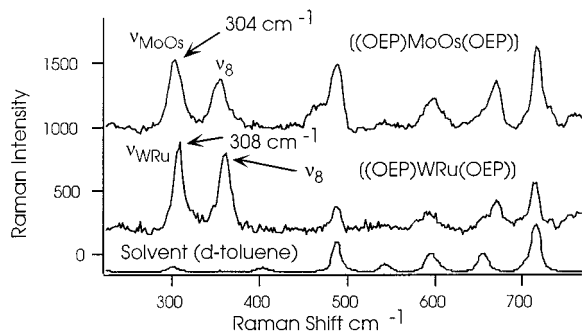
(10) Antipas, A.; Buchler, J. W.; Gouterman, M.; Smith, P. D. *J. Am. Chem. Soc.* **1978**, *100*, 3015–3024.

(11) Evans, D. F. *J. Chem. Soc.* **1959**, 2003–2005.

Table 1. ^1H NMR^a and Magnetic Susceptibility^b of d¹⁰ Metal–Metal-Bonded Porphyrin Dimers

dimer	μ_{eff} (μ_{B})	$\delta(\text{H}_{\text{meso}})$ (s)	$\delta(-\text{CH}_2)$ (q)	$\delta(-\text{CH}_3)$ (t)
$[\text{Re}(\text{OEP})_2]$	$\leq 0.8^c$	6.45 (s)	3.73, 3.98	1.65
$[(\text{OEP})\text{MoOs}(\text{OEP})]$	2.72	-50.93 (Mo) -67.92 (Os)	9.20, 10.31 (Os) 16.7, 20.4 (Mo)	0.87 (Os) 0.20 (Mo)
$[(\text{OEP})\text{WRu}(\text{OEP})]$	2.80	-16.10 (Ru) -90.0 (W)	6.40, 7.08 (Ru) 20.5, 23.9 (W)	1.95 (Ru) -0.80 (W)

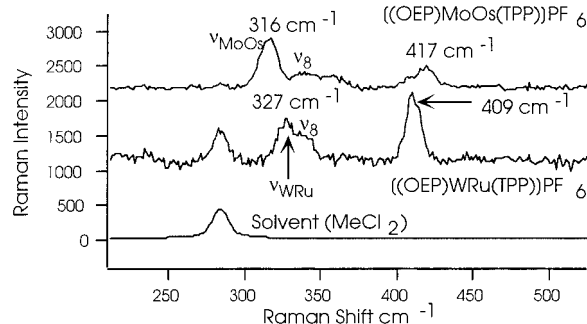
^a All spectra taken in toluene-*d*₈. ^b Evans method in toluene-*d*₈ at 20 °C. ^c No effect observed.

**Figure 1.** Low-frequency RR spectra upon excitation at 363.8 nm for **3** and **4**. Samples were prepared in toluene-*d*₈ solution and flame sealed. Solvent resonances were not subtracted from the raw data but are given for comparison. All spectra are baseline corrected. Sample stability was confirmed by ^1H NMR analysis following excitation.

The chemical shift data in Table 1 also imply that the WRu dimer exhibits a significantly more polarized metal–metal bond than does the MoOs dimer, as would be expected from the relative positions of the metals in the periodic table. The W(OEP) resonances exhibit much larger isotropic shifts than do the corresponding Ru(OEP) resonances in **4**, suggesting that the antibonding HOMO (containing the 2 unpaired electrons) in the WRu dimer is predominantly W in character. In contrast, the MoOs dimer exhibits comparable isotropic shifts for both halves of the dimer, consistent with a much closer match of electronegativities for Mo and Os. To date we have not yet been able to directly measure the dipole moments in the two dimers, but such an experiment is expected to demonstrate a significantly larger dipole moment for WRu.

Vibrational Spectroscopy. Experimental difficulty has thus far prevented us from obtaining thermochemical data in an attempt to compare metal–metal bond enthalpies in these and similar complexes. However, the metal–metal bond force constants from two sets of analogous MoOs and WRu porphyrin dimers have been obtained with resonance Raman vibrational spectroscopy (Figures 1 and 2) and provide reasonable estimates for the relative metal–metal bond strengths.¹²

Resonance enhancement of the metal–metal stretching vibration in the neutral dimers $[(\text{OEP})\text{MoOs}(\text{OEP})]$ (**3**) and $[(\text{OEP})\text{WRu}(\text{OEP})]$ (**4**), as well as in the monocations $[(\text{OEP})\text{MoOs}(\text{TPP})]\text{PF}_6$ (**5**⁺) and $[(\text{OEP})\text{WRu}(\text{TPP})]\text{PF}_6$ (**6**⁺), has been achieved with UV excitation at 363.8 nm. For the neutral complexes (Figure 1), only two low-frequency bands were observed for each dimer. On the basis of normal coordinate analyses of $[(\text{OEP})\text{MM}'(\text{OEP})]^{2b}$ and NiOEP,¹³ the bands near 350 cm⁻¹ may be assigned as ν_8 , an OEP core-breathing mode (23% C_αC_mC_α, 18% ν_{MN} , 16% $\nu_{\text{C}_\alpha\text{C}_\beta}$, 12% $\delta_{\text{C}_\alpha\text{NC}_\alpha}$).¹⁴ The remaining bands near 300 cm⁻¹ are assigned as ν_{MM} , consistent

**Figure 2.** Low-frequency RR spectra upon excitation at 363.8 nm for **5**⁺ and **6**⁺. Assignment of the bands near 345 cm⁻¹ to OEP-based breathing modes was made according to the descriptions of ν_8 and ν_{35} in ref 13. An analogous mode for TPP core-breathing is expected near 410 cm⁻¹ (ref 14), and the observed bands at 408 and 417 cm⁻¹ have been thus assigned.**Table 2.** Vibrational Data for MoOs and WRu Metal–Metal-Bonded Porphyrin Dimers

dimer	ν_{MM} (cm ⁻¹)	k (mdyn/Å)	bond order
$[(\text{OEP})\text{MoOs}(\text{OEP})]$	304	3.47	3.0
$[(\text{OEP})\text{WRu}(\text{OEP})]$	308	3.65	3.0
$[(\text{OEP})\text{MoOs}(\text{TPP})]\text{PF}_6$	316	3.75	3.5
$[(\text{OEP})\text{WRu}(\text{TPP})]\text{PF}_6$	327	4.11	3.5

with the depolarization ratios and subtraction of monomeric spectra. Similarly, the spectra in Figure 2 may be assigned with ν_{MM} , ν_8 , and a metal–TPP core-breathing mode analogous to ν_8 . The TPP breathing mode (19% δMNC_α , 17% $\nu_{\text{C}_m\text{C}_{\text{Ph}}}$, 16% δMNC_α , 14% $\text{C}_{\text{Ph}}\text{C}_{\text{Ph}}\text{C}_{\text{Ph}}$)¹⁴ is predicted to exist near 410 cm⁻¹, and bands are seen at 409 cm⁻¹ (WRu⁵⁺) and 417 cm⁻¹ (MoOs⁵⁺). The existence of a similar band for $[(\text{OEP})\text{MoRu}(\text{TPP})]\text{PF}_6$ at 408 cm⁻¹ lends further support to this assignment. The location of ν_8 is expected between 340 and 360 cm⁻¹, and corresponding features are seen at 340 cm⁻¹ (WRu⁵⁺) and 341 cm⁻¹ (very weak, MoOs⁵⁺). The only remaining nonsolvent bands, at 316 cm⁻¹ (MoOs⁵⁺) and 327 cm⁻¹ (WRu⁵⁺), are now assigned as ν_{MM} . Enhancement of the metal–metal stretches via Soret excitation is consistent with numerous existing reports and has been previously discussed at length.^{2b}

Force constants associated with each metal–metal bond have been calculated with the diatomic oscillator approximation¹⁵ and are presented in Table 2. The force constants for these dimers, each containing one 4d metal and one 5d metal, are intermediate to the force constants obtained for analogous 4d–4d (MoRu) and 5d–5d (WOs) dimers. Comparisons between the MoOs and WRu dimers indicate that the WRu metal–metal bonds may be slightly *stronger* than corresponding MoOs bonds, but the differences are small and may be the result of influences outside the diatomic oscillator approximation.¹⁶

(13) (a) Kitagawa, T.; Abe, M.; Ogoshi, H. *J. Chem. Phys.* **1978**, *69*, 4516–4525. (b) Abe, M.; Kitagawa, T.; Kyogoku, Y. *J. Chem. Phys.* **1978**, *69*, 4526–4534.

(14) Atamian, M.; Donohoe, R. J.; Lindsey, J. S.; Bocian, D. F. *J. Phys. Chem.* **1989**, *93*, 2236–2243.

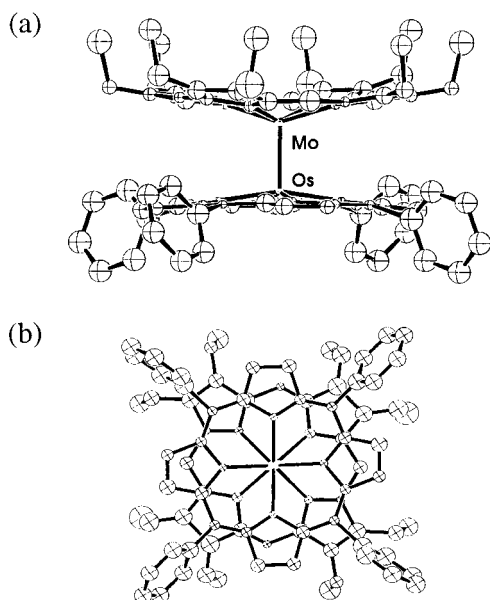
(15) $k = (3.55 \times 10^{17})\mu\nu^2$, where k = force constant (mdyn/Å), μ = reduced mass of the two metal atoms (g), and ν = vibrational frequency (cm⁻¹).

(16) Our analysis assumes the metal–metal bond stretches to be purely diatomic, but they may contain a small dependence on metal–metal–N bending, metal–N stretching, or other ligand-based modes. We have published a simple normal coordinate analysis (ref 2b, Supporting Information) for vibrational study of metalloporphyrin dimers, and our results indicate a metal–metal stretch which is ca. 90% diatomic for these complexes. Thus, the small difference between observed force constants for MoOs and WRu dimers may not reflect a stronger bond for WRu.

(12) Cotton, F. A.; Walton, R. A. *Multiple Bonds Between Metal Atoms*, 2nd ed.; Clarendon Press: Oxford, U.K., 1993.

Table 3. Selected Structural Parameters (Å) for [(OEP)MoOs(TPP)]PF₆ (**5**⁺) and [(OEP)WRu(TPP)]PF₆ (**6**⁺)

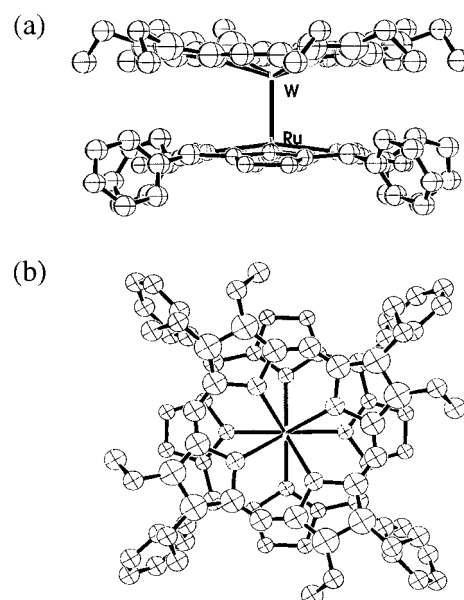
	M–M'	Mo–N ₄ or W–N ₄	Os–N ₄ or Ru–N' ₄	N ₄ –N' ₄	N–M–M'–N' ₄ dihedral angle ^a	MO diagram (bond order)
5 ⁺	2.238(3)	0.581(4)	0.309(4)	3.14(1)	42.1	$\sigma^2\pi^4\delta^2\pi^*1$ (3.5)
6 ⁺	2.297(2)	0.609(4)	0.294(4)	3.20(1)	29.9	$\sigma^2\pi^4\delta^2\pi^*1$ (3.5)

^a Geometric mean given in deg.**Figure 3.** (a) 50% probability ORTEP plot of **5**⁺: Mo–Os = 2.238(3) Å; N₄–N'₄ = 3.14 Å; Mo–N₄ = 0.581 Å; Os–N'₄ = 0.309 Å. (b) ORTEP plot of **5**⁺ as viewed down the Mo–Os bond axis: porphyrin cores are rotated 42.1°.

X-ray Crystallography. The monocationic complexes [(OEP)MoOs(TPP)]PF₆ (**5**⁺) and [(OEP)WRu(TPP)]PF₆ (**6**⁺) have been structurally characterized by X-ray diffraction. Attempts to obtain X-ray-quality single crystals of the corresponding neutral complexes have so far been unsuccessful.

Surprisingly, the X-ray structures of **5**⁺ (Figure 3) and **6**⁺ (Figure 4) display more differences than similarities. Whereas **5**⁺ crystallized in the space group *Pnma* (No. 52), **6**⁺ crystallized in an altogether different group, *P4/nmm* (No. 129). The porphyrin–porphyrin twist angles (χ) are also significantly different; the WRu compound exhibits a mean N–W–Ru–N' dihedral angle of 29.9°, while the MoOs entity is closer to the perfectly staggered conformation with a mean N–Mo–Os–N' angle of 42.1°. These twist angles imply a stronger δ bond for WRu,¹⁷ but because the MoOs bond is significantly shorter, the relative extents of δ overlap are not absolutely clear. Furthermore, the likely possibility that crystal packing forces might influence the molecular geometry and induce these subtle differences in conformation and metal–metal separation should not be ignored.

Other interesting features of the two structures are the metal–N₄ displacements and N₄–N'₄ separations (Table 3). For the MoOs compound, the porphyrin–porphyrin separation is slightly decreased from the value seen in WRu. This situation is

**Figure 4.** (a) 50% probability ORTEP plot of **6**⁺: W–Ru = 2.297(2) Å; N₄–N'₄ = 3.20 Å; W–N₄ = 0.609 Å; Ru–N'₄ = 0.294 Å. (b) ORTEP plot of **6**⁺ as viewed down the W–Ru bond axis: porphyrin cores are rotated 29.9°.

analogous to that reported for the two conformations exhibited in the structure of [(OEP)MoRu(TPP)]PF₆; in each case tighter internal angles of rotation are seen to associate with longer porphyrin–porphyrin separations. The inverse correlation of porphyrin–porphyrin separation with internal twist angle is most likely a result of the increased nonbonded repulsions incurred by the more eclipsed conformations.

Interestingly, the sums of metal–N₄ displacements in both **5**⁺ and **6**⁺ are nearly identical—0.89 Å (Mo–N₄ + Os–N'₄) and 0.90 Å (W–N₄ + Ru–N'₄). Because of this similarity, the shorter N₄–N'₄ separation (by 0.06 Å) for the Mo–Os dimer translates into a shorter metal–metal bond length. Although it is often tempting to invoke the traditional correlation between bond length and bond strength, these heterodimeric compounds indicate that a variety of factors contribute to the determination of an equilibrium metal–metal separation. For example, the W–Ru bond may be longer because it is inherently weaker, but there is also the possibility that crystal packing forces impart a more eclipsed geometry on the ligands, forcing them to elongate and stretch the W–Ru bond. Thus, the solid-state characterizations of MoOs and WRu may not enable any direct conclusions about the relative bond strengths for these MoOs and WRu species.

Conclusions

¹H NMR, vibrational, and X-ray spectroscopy have been utilized to characterize several intertriad heterodimeric MoOs and WRu porphyrin complexes. A molecular orbital description, $\sigma^2\pi^4\delta^2\pi^*2$, is implied by the magnetic properties of the neutral species and structural conformation of the corresponding monocations. Extremely weak δ -bonding interactions (<5 kcal/

(17) The observed N–M–M'–N' angles of 29.9° (WRu) and 42.1° (MoOs) imply δ -bond strengths of approximately 25% and 10%, respectively, of the maximum interaction energy with N–M–M'–N' = 0.0° and the same metal–metal distance in both cases. Estimation of the δ -bond strengths for several eclipsed Mo₂, MoW, and W₂ species has been achieved by dynamic NMR and provides values of ca. 10 kcal/mol: (a) Collman, J. P.; Garner, J. M.; Hembre, R. T.; Ha, Y. *J. Am. Chem. Soc.* **1992**, *114*, 1292. (b) Kim, J. C.; Goedken, V. L.; Lee, B. M. *Polyhedron* **1996**, *15*, 57–62.

mol), if any, are indicated by the dihedral angles of [(OEP)-MoOs(TPP)]PF₆ (42.1°) and [(OEP)WRu(TPP)]PF₆ (29.9°), respectively. Comparison of the bond lengths and force constants for several WRu and MoOs species indicates that their bond strengths are nearly identical. Although two independent sets of resonance Raman data produce force constants which are 5–10% larger for WRu species, the difference is small enough that we may not confidently conclude the existence of a significantly stronger bond for WRu. Likewise, the bond length of a MoOs dimer is seen to be 0.05 Å shorter than the corresponding WRu complex, suggesting that the MoOs bond might be stronger. These data indicate that steric factors may play an important role in the exact description of the complexes and that their metal–metal bond strengths are similar. The existence of a “special stability” associated with the more polar WRu bond is therefore not clear, and we are considering further studies (EAS, PES)¹⁸ in order to further address the situation.

Acknowledgment. We thank the NSF (Grant CHE 9123187-A4) for financial support. Special thanks to Dr. Doris Hung at Northwestern for mass spectra, Dr. Fred Hollander at the University of California at Berkeley for X-ray data collection, and Pharmacyclics for their generous gift of diethylpyrrole used in the synthesis of H₂OEP. S.F. and A.P.S. are grateful for the support of a Director’s Fellowship from Los Alamos National Laboratory.

Supporting Information Available: Tables of structural parameters for **5**⁺ and **6**⁺. This material is available free of charge via the Internet at <http://pubs.acs.org>.

IC9810337

(18) Bursten, B. E.; Cotton, F. A.; Cowley, A. H.; Hanson, B. E.; Lattman, M.; Stanley, G. G. *J. Am. Chem. Soc.* **1979**, *101*, 6244.